DISTRIBUTION OF ELEMENTS IN HIGH-ENTROPY CoCrFeNi AND NbTaTiV ALLOYS IRRADIATED WITH LOW-ENERGY Kr IONS

V.V. Uglov[1], N.A. Stepanjuk[1], I.V. Safronov[1], S.V. Zlotski[1], I.A. Ivanov[2,3], A.E. Ryskulov[2], A.E. Kurakhmedov[2], A.L. Kozlovskiy[2,3], M.V. Zdorovets[2,3], K. Jin[4]

[1]Belarusian State University, 4 Nezavisimosty ave., 220030 Minsk, Belarus
[2]Institute of Nuclear Physics, Abylai Khan str., 2/1, 010008 Nur-Sultan, Kazakhstan
[3]L.N. Gumilyov Eurasian National University, Satpayev Str., 2, 010008 Nur-Sultan, Kazakhstan
[4]Beijing Institute of Technology, 5 South Street, Zhongguancun, Haidian District, 100081 Beijing, China

Modern challenges in the fields of nuclear energy are concentrated greatly across the increment of power and efficiency of nuclear facilities by increasing their working temperatures [1–3]. Classical materials, such as steels (including austenitic), nickel and other metal alloys with a binary base, are facing phase transformations and significant degradation of physical and mechanical properties at elevated temperatures, corroding when in contact with liquid coolants and some gases, and swelling under high doses of neutron irradiation [2–3].

One of the most perspective classes of materials for the aims named upper can be high-entropy alloys (HEAs) [1–7]. The vanguard works on the theme of high-entropy alloys belong to Senkov and Kantor [8, 9]. HEAs mostly form single-phased either FCC (transitive 3d-metals) or BCC (refractory metals) distorted crystal lattice with disordered element location, which is the reason of their elevated thermal stability, corrosion and radiation resistance [10].

The cuboid samples with linear dimensions of 5×5×1.5 mm for CoCrFeNi and 6×6×1 mm for NbTaTiV were prepared in Beijing Institute of Technology by arc melting in argon atmosphere from high-purity (>99,97%) constituent metal powders. After casting into copper mould ingots were annealed at 1150 °C for 24 h, cold-rolled till 85% thickness reduction and again annealed at 1150 °C for 72 h. The samples were irradiated in Astana Branch of Institute of Nuclear Physics Institute on DC-60 heavy ion accelerator with Kr^{14+} ions, energy 280 keV, fluence 5×10^{15} cm^{-2}. Heavy ion Rutherford backscattering (HIRBS) experiment was performed on the same installation using $^{14}N^{2+}$ ions with energy of 14 MeV.

The HIRBS spectra of non-irradiated and krypton ion irradiated HEAs samples are performed on Fig. 1-2. They show, that in non-irradiated samples of CoCrFeNi and NbTaTiV HEAs takes place relatively uniform elemental depth composition, the results of mathematical simulation are shown on Table 1.

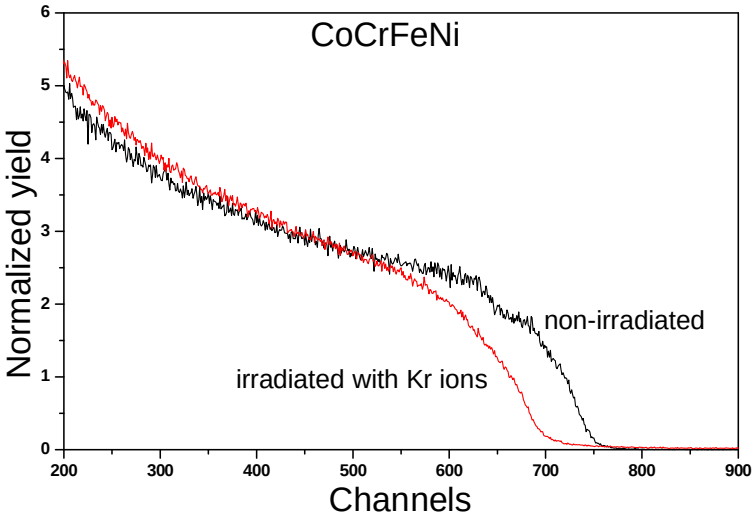

Fig. 1. HIRBS spectra of non-irradiated and irradiated with Kr14, 40 keV CoCrFeNi HEAs

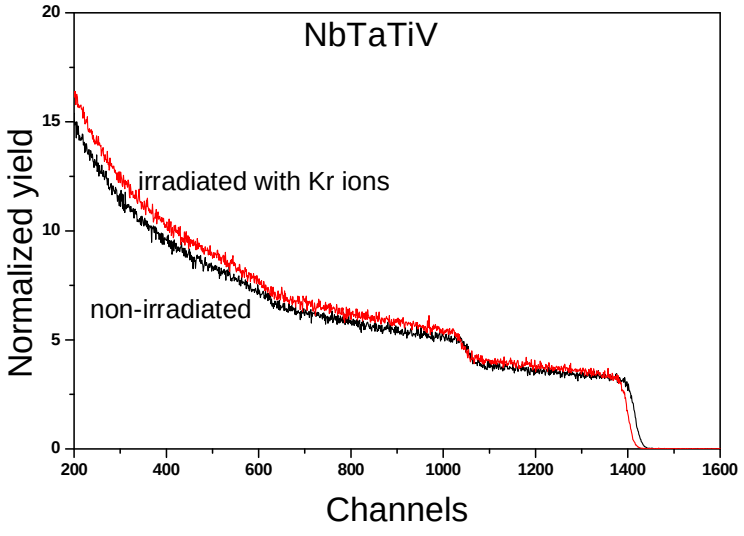

Fig. 2. HIRBS spectra of non-irradiated and irradiated with Kr14, 40 keV NbTaTiV HEAs

In case of NbTaTiV irradiation caused no significant changes in HIRBS spectrum profile. But in CoCrFeNi alloy irradiation with crypton led to rearranging of elements with depth. The plot of elemental composition, obtained from simulation results, is introduced on Fig. 3.

Table 1. Elemental composition of non-irradiated CoCrFeNi and NbTaTiV HEAs samples (HIRBS)

Composition, at. %	Co	Cr	Fe	Ni	Nb	Ta	Ti	V
CoCrFeNi	28,9	26,0	26,2	17,9	-	-	-	-
NbTaTiV	-	-	-	-	30,0	30,0	20,4	19,6

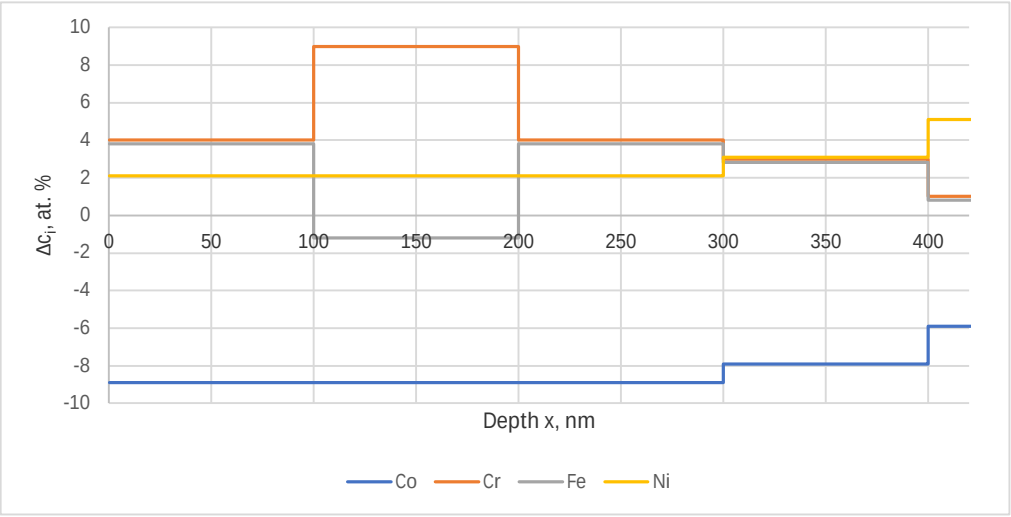

Fig. 3. Depth profile of elements of CoCrFeNi HEA after Kr irradiation

As seen on Fig. 3, irradiation led to decrease of Co concentration on nearly 9 at. % till the depth of 300 nm. All the other element concentration increased. In Cr distribution there is a + 9 at. % maximum on the depth from 100 nm till 200 nm, which fully correlates with -1 at. % minimum of Fe concentration.

Correlative plot of damage dose and implanted Kr concentration, calculated from SRIM data, and dislocation density depth distribution, calculated from XRD spectra with Williamson-Hall uniform deformation model, are represented on Fig. 4. Evidently, takes place some kind of irradiation defect annealing and crystalline size increase in the region near the maximum implanted Kr, where usually situated maximal amount of voids and bubbles. Dislocation density there is decreased on 8×10^{12} cm^{-2} compared with non-irradiated sample. Maximum of

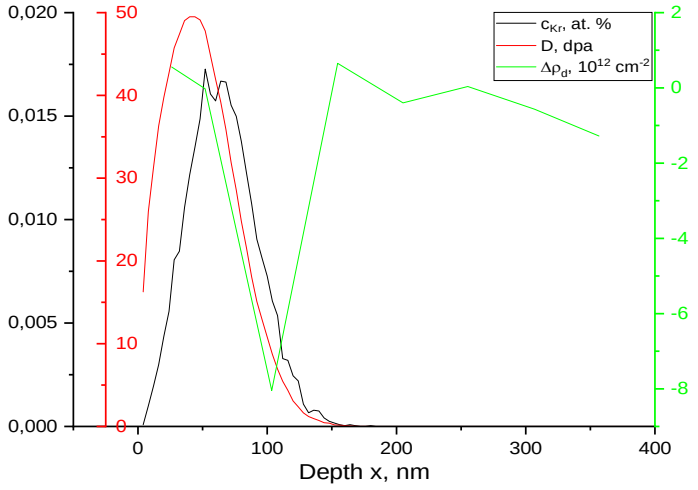

Fig. 4. Depth profile of concentration of implanted Kr, damage dose and dislocation density change after Kr irradiation of CoCrFeNi HEA

chromium and minimum of iron distribution occurs in the region behind the minimum of dislocation density change, which can be the consequence of radiation-induced diffusion and movement of crystalline borders.

Element composition in irradiated region of CoCrFeNi shows redistribution with cobalt depletion and enrichment of chromium and nickel. Iron is depleted mainly in region of dislocation density minimum, where chromium is mostly enriched by irradiation defect annealing. But in NbTaTiV there is no redistribution observed, which tells about better irradiation induced diffusion suppression in BCC-latticed HEA. Probable reason for such behavior can be lack of crystal lattice symmetry in BCC lattice in comparison with FCC lattice and greater atomic radii of Nb and Ta, providing greater crystal lattice distortion of NbTaTiV compared with CoCrFeNi. All these results lead to the hypothesis of better irradiation phase and structural stability of BCC HEAs upon FCC ones in case of ion irradiation with low implanted Kr concentration and higher damage doses, while free vacancies and voids prevail on gas-vacancy complexes and gas bubbles.

Acknowledgements. This work was financially supported by State Program of scientific research “Energy and nuclear processes and technologies” (2.1.03.2) and Ministry of Education and Science of the Republic of Kazakhstan Science Committee (grant No. AP14872199).

References

1. **Y. F. Ye, Q. Wang, J. Lu, C. T. Liu, Y. Yang** Progress in Materials Science, Materials Today, (2015) 1 – 14.
2. **A. M. Manzoni, U. Glatzel** Encyclopedia of Materials: Metals and Alloys, (2020).
3. **W. Li, D. Xie, D. Li, Y. Zhang, Y. Gao, P.K. Liaw.** Progress in Materials Science, 118 (2021) 100777.
4. **S. Son, S. Kim, J. Kwak, G.H. Gu, D.S. Hwang, Y.T. Kim, H.S. Kim** Materials Letters, 300 (2021) 130130.
5. **P. F. Yu, L. J. Zhang, H. Cheng, H. Zhang, M. Z. Ma, Y.C. Li, G. Li, P.K. Liaw, R.P. Liu** Intermetallics, 70 (2016) 82 – 87.
6. **N.E. Koval, J.I. Juaristi, R.D. Muiño, M. Alducin** Journal of Applied Physics, 127 (2020) 145102.
7. **Y. Zhang, T.T. Zuo, Z. Tang, M.C. Gao, K.A. Dahmen, P.K. Liaw, Z.P. Lu** Progress in Materials Science 6 (2014) 1 – 93.
8. **B. Cantor, I.T.H. Chang, P. Knight, A.J.B. Vincent** Materials Science Eng., 375 (2004) 213-218
9. **O.N. Senkov, J.M. Scott, S.V. Senkova, D.B. Miracle, C.F. Woodward** Journal of Alloys and Compounds, 509 (2011) 6043–6048.
10. **A.S. Rogachev** Metal physics and metal science, 121 (2020) 807 – 841 (in Russian).